CHEMICAL ENGINEERING TRANSACTIONS
VOL. 33, 2013
A publication of AIDIC
The Italian Association of Chemical Engineering
Online at: www.aidic.it/cet
Guest Editors: Enrico Zio, Piero Baraldi

ISBN 978-88-95608-24-2; **ISSN** 1974-9791
DOI: 10.3303/CET1333158

Thermal-Electrochemical Modeling and Parameter Sensitivity Analysis of Lithium-ion Battery

Liqiang Zhang, Chao Lyu*, Lixin Wang, Weilin Luo, Kehua Ma

School of Electrical Engineering and Automation, Harbin Institute of Technology, No.92 West Dazhi Street, Nangang District, 150001 Harbin, China
lu_chao@hit.edu.cn

In this paper, a thermal-electrochemical model of Li-ion battery was developed based on P2D model, and a set of parameters which related to PHM characteristics were proposed along with the parameter sensitivity analysis. Sensitivity value matrixes were also presented to describe the sensitivity of model output when parameters take different values on different operating conditions. Then, parameters were clustered into four clusters using fuzzy clustering method according to their "Best Condition for Identification", on which the parameter has the greatest sensitivity and most easily to be identified. Finally, design criteria and application suggestions of the "Best Practicable Conditions" were also discussed.

1. Introduction

The ultimate purpose of our research is to build a PHM characteristics library of Li-ion battery by finding out which parameters will change and how they change in different aging patterns. The core work is to develop a numerical model which can predict the battery behavior, and identify the model parameters which are treated as internal characteristics accurately.

Marc et al. (1993) developed a fundamental pseudo 2-dimension (P2D) numerical model of Li-ion battery, including electronic charge balance, mass balance and electrochemical kinetics parts. Model parameters are not only the important inputs of model simulation, but also the indicators of the state of health (Zhang and Ralph, 2008). Because it is very difficult to identify the large amount of parameters quickly and accurately, a step-by-step method along with parameter sensitivity analysis (Alexander et al., 2010) was proposed. Joel et al. (2012) used Fisher information matrix to estimate the parameters identifiability, but it is very complex for thermal-electrochemical model. Wang et al. (2012) used model simulation to exam parameter sensitivity and Srinivasulu et al. (2011) provided a simple method based on simulated curves to quantify the parameter sensitivity for PEM fuel cell model. All of them have roughly classified the parameters into several groups according to their sensitivity. Moreover, there are few established standards of identification experiments, constant current and standard dynamic tests are usually used by researchers.

The main research of this paper is to couple the P2D model to the thermal model, and propose a sensitivity value matrix to relate the parameters' sensitivity to operating conditions, then use it for parameter clustering and guide the design of "Best Practicable Conditions".

2. Modeling

2.1 Electrochemical part

Figure 1 shows a published schematic of Li_xC_6/Li_yFePO_4 battery. The P2D model assumes that the active material of both electrodes is spherical. In discharge process, the Li^+ deinserts from active material to electrolyte, then moves from the anode to the cathode, where electrons (e^-) return closing the electric circuit, and inserts into cathode active material. In charge process the Li^+ moves backwards. This phenomenon is known as "rocking chair". Two electrode/separator interface (boundary 2 and 3) and two electrode/current collector interface (boundary 1 and 4) are also shown.

Please cite this article as: Zhang L., Lyu C., Wang L., Luo W., Ma K., 2013, Thermal-electrochemical modeling and parameter sensitivity analysis of lithium-ion battery, Chemical Engineering Transactions, 33, 943-948 DOI: 10.3303/CET1333158

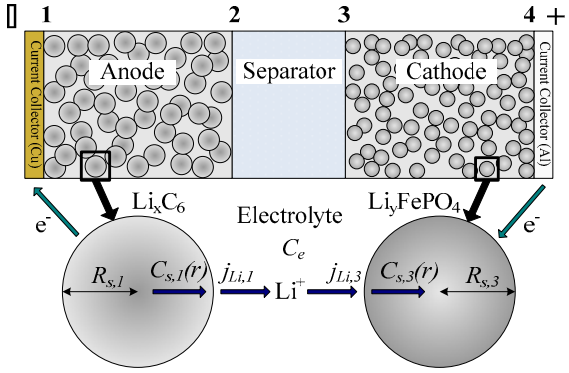

Figure 1: Schematic of Li-ion battery.

Faraday's laws express the relationship between the pore-wall flux of Li-ion at the surface of active material and the electrical charge flow, according to the law of conservation of charge:

$$\nabla \cdot \mathbf{I}_2 = a_s i_s = a_s F j_{Li}; \quad \nabla \cdot \mathbf{I}_1 = -a_s i_s = -a_s F j_{Li}; \quad \mathbf{I}_1 + \mathbf{I}_2 = \mathbf{I}; \quad \nabla \cdot (\mathbf{I}_1 + \mathbf{I}_2) = 0 \tag{1}$$

$\mathbf{I}_2$ and $\mathbf{I}_1$ are current density of Li^+ and electron, $a_s=3\varepsilon_s/R_s$ is the specific area of the active material, ε_s is the volume fraction of the active material, and R_s is the radius of electrode spherical particle. The electron current density is zero at the boundary 2 and 3, while it is equal to the total current density $\mathbf{I}$ at the boundary 1 and 4.
Charge balance and Ohm's law are used to show the relationship of current density and potential:

$$\begin{cases} \mathbf{I}_1 = -\sigma_s^{eff} \nabla \phi_s \\ \mathbf{I}_2 = -\kappa_e^{eff} \nabla \phi_e + \dfrac{2\kappa_e^{eff} RT}{F}(1 + \dfrac{\partial \ln f_{\pm}}{\partial \ln C_e})(1 - t_+^0) \nabla \ln C_e \end{cases} \tag{2}$$

$\sigma_s^{eff} = \sigma_s \varepsilon_s^{1.5}$ is the effective electronic conductivity, $\kappa_e^{eff} = \kappa_e \varepsilon_e^{1.5}$ is the effective ionic conductivity of electrolyte, C_e stands for the electrolyte concentration. ϕ_s is 0 at boundary 1, the charge flux is set to be equal to $\mathbf{I}$ at boundary 4, and is isolation at boundary 2 and 3. Since there is no charge flux, ϕ_e is taken to be continuous at boundary 2 and 3, while it is set as isolation at boundary 1 and 4.
The solution phase concentration in electrolyte is given by mass balance:

$$\varepsilon_e \frac{\partial C_e}{\partial t} = \nabla \cdot (D_e^{eff} \nabla C_e) + \frac{a_s}{F}(1 - t_+^0) \cdot i_s \tag{3}$$

$D_e^{eff} = D_e \varepsilon_e^{1.5}$ is the effective diffusion coefficient of Li^+; t_+^0 is the transference number. The boundary conditions of C_e is set to be continuous at boundary 2 and 3, the flux of Li^+ is set to 0 at boundary 1 and 4.
The mass balance of Li^+ in a particle of electrode active material is described by Fick's law:

$$\frac{\partial C_s}{\partial t} = \frac{1}{r^2} \nabla \cdot (D_s r^2 \nabla C_s) \tag{4}$$

C_s is the concentration of Li^+ in active material, D_s is the Li^+ diffusion coefficient in solid phase. The Li^+ flux at the surface of particle is equal to the j_{Li} in (1), and there is no flux in the center of sphere.
The electrochemical reaction which occurs at the interface can be given by Butler-Volmer equation:

$$j_{Li} = k_s C_e^{0.5} (C_{s,MAX} - C_{e/s})^{0.5} C_{e/s}^{0.5} [\exp(\frac{0.5F}{RT}\eta) - \exp(-\frac{0.5F}{RT}\eta)] \tag{5}$$

k_s is the reaction rate, $C_{e/s}$ is the Li^+ concentration at the reaction interface. The reaction is driven by over potential η, which defined as $\eta = \phi_s - \phi_e - E_{ocv} - i_s R_{film}$. R_{film} is the film resistance; E_{ocv} is the open-circuit potentials which determined by Li^+ insert rate in active material.
The terminal voltage, which is also the output of the model, is determined by the different solid phase potentials between boundary 1 and 4 and the extra resistance in the battery: $U_{app} = \phi_s\big|_4 - \phi_s\big|_1 - |\mathbf{I}| R_{ext}$.

2.2 Thermal part

For a small battery, the energy balance equation can be written as:

$$\rho C_p \frac{\partial T}{\partial t} = \dot{Q} - \dot{q} \tag{6}$$

where ρ is the volume averaged density and C_p is the averaged heat capacity of the battery. There is no heat conduction term in (6) because temperature gradient affects the model output very little in a small cell. The local heat generation which includes active heat, reaction heat, ohmic heat and extra heat is:

$$\dot{Q} = a_s i_s (\phi_s - \phi_e - E_{ocv} + T\frac{dE_{ocv}}{dT}) + (\sigma_s^{eff}\nabla\phi_s\nabla\phi_s + \kappa_e^{eff}\nabla\phi_e\nabla\phi_e + \kappa_e^{D,eff}\nabla\ln C_e\nabla\phi_e) + \frac{|\mathbf{I}|^2 R_{ext}}{L} \tag{7}$$

The heat exchange between the battery and ambient was given as follow, according to Newton's cooling law and radiation law:

$$\dot{q} = h(T - T_a) + \sigma\varepsilon(T^4 - T_a^4) \tag{8}$$

h is the heat transfer coefficient; σ is the Stefan-Boltzmann constant; ε is the blackness of battery surface; T_a is ambient temperature.

The Arrhenius' law was used to couple the electrochemical parameters in P2D model to the thermal part:

$$X_i = X_{i,ref}\exp[\frac{E_i}{R}(\frac{1}{T_{ref}} - \frac{1}{T})] \tag{9}$$

In this case, X_i is a general variable representing the diffusing coefficient D_s, the reaction rate k_s of electrode active material, the diffusing coefficient D_e, and the conductivity κ_e of electrolyte. $X_{i,ref}$ is the parameter value at the reference temperature T_{ref}, and E_i is the activation energy.

In thermal-electrochemical coupled model, battery temperature can be calculated based on P2D model. Meanwhile, some parameters of P2D model are determined by the temperature.

2.3 Model simulation

A full set of parameters of a 2.3 Ah $LiFePO_4$ cylindrical 26650 type battery was used in this paper for simulation and parameters sensitivity analysis. These parameters were given by Safari et al. (2011) and Prada et al. (2012), including the geometry, kinetic and transport parameters and thermal parameters.

We have improved the DUALFOIL5.1 program (original source code was from Newman's group) and used it for simulation. Heat generation, temperature and thermal-electrochemical coupling subroutine was added in. the output of the model is terminal voltage and input is the parameters and operating conditions.

3. Parameters sensitivity analysis and discussion

3.1 Subset of parameters and methodology

Not all parameters need to be identified by using the numerical model. Some parameters are changeless during cycling or can be got directly, such as the geometry parameters or material characteristics. A set of 28 parameters, which will be identified by a non-invasive method, is proposed and divided into 2 groups:

Group 1 includes 17 parameters. They are the radius of active particle $R_{s,a}$ and $R_{s,c}$, the diffusion coefficient in solid phase $D_{s,a}$ and $D_{s,c}$, the electronic conductivity of solid $\sigma_{s,a}$ and $\sigma_{s,c}$, the initial soc x_0 and y_0, the volume fraction of the active material $\varepsilon_{s,a}$ and $\varepsilon_{s,c}$, the film resistance $R_{film,a}$ and $R_{film,c}$. The subscript a and c stands for anode and cathode, respectively. In addition, the concentration C_e, the diffusion coefficient D_e, the ionic conductivity κ_e, the density ρ_e of electrolyte and the extra resistance R_{ext} are also in this group. These 17 parameters indicate the basic properties of the battery, and probably change when battery degenerates, so we treat them as internal characteristics in PHM characteristics library.

Group 2 includes 11 parameters, they are the solution volume fractions $\varepsilon_{e,a}$, $\varepsilon_{e,c}$ and $\varepsilon_{e,s}$, the reaction rate $k_{s,a}$ and $k_{s,c}$, and the activation energy in Arrhenius' law including $\bar{E}k_{s,a}$, $\bar{E}k_{s,c}$, $\bar{E}D_{s,a}$, $\bar{E}D_{s,c}$, $\bar{E}D_e$, and $\bar{E}\kappa_e$. These parameters may not change during degradation but difficult to be got directly.

In individual parameter sensitivity analysis, five values for each parameter were chosen in a range to analyze the influence of the parameter on discharge curve in different conditions with the other parameters equal to benchmark value. The value ranges of parameters are shown in column "Range" of Table 1, considering the benchmark value from different references and the probable variation trend during the aging process. The battery model with different parameter values were simulated discharging from its fully charged state to its fully discharged state at five different ambient temperature (-5 °C, 10 °C, 25 °C, 40 °C,

55 °C) and five different discharge rate (0.2C, 0.5C, 1C, 2C, 4C) respectively. So, 25 combination operating conditions were represented in this paper. Figure 2 shows the curves of parameter $R_{s,a}$ and $\bar{E}k_{s,c}$ with five value on a certain condition, the dispersion of curves indicates the parameter sensitivity.

3.2 Quantifying and sensitivity value matrix

First, the standard deviation of U_{app} at each dod point for a parameter was determined as follow:

$$SU(dod, j, i) = \underset{k}{\text{std}}(U_{app}(dod, k, j, i)) \tag{10}$$

where $U_{app}(dod,k,j,i)$ stands for the terminal voltage at dod^{th} point on discharge curve with the k^{th} value of the parameter which to be analyzed, at the j^{th} ambient temperature and i^{th} discharge rate.
Secondly, the mean of standard deviations was calculated in four range of dod respectively, and the standard deviation of EOD points was used to calculate the sensitivity at the end of discharge:

$$\begin{cases} SMU(1, j, i) = \underset{0<dod<0.2}{\text{mean}}\,[SU(dod, j, i)] \\ SMU(2, j, i) = \underset{0.2<dod<0.4}{\text{mean}}\,[SU(dod, j, i)] \\ SMU(3, j, i) = \underset{0.4<dod<0.6}{\text{mean}}\,[SU(dod, j, i)] \\ SMU(4, j, i) = \underset{0.6<dod<0.8}{\text{mean}}\,[SU(dod, j, i)] \\ SMU(5, j, i) = \underset{k}{\text{std}}(k, EOD) \end{cases} \tag{11}$$

Finally, a 3-D matrix $SMU(d,j,i)$ which is called the “sensitivity value matrix” were obtained using Eq. (10) and (11) on 25 combination conditions we have chosen. Each element in this matrix means the parameter sensitivity at a certain DOD range, ambient temperature and discharge rate. The sensitivity value matrixes of 28 parameters were calculated by this method. Figure 3 shows the sensitivity value matrix of parameter $R_{s,a}$ and $R_{film,c}$. And the column “SMU_{avg}” in Table 1 shows the mean value of all elements in the matrix for each parameter. The parameters which mean sensitivity greater than 0.01 were grouped as “Highly Sensitive (**)”, those lower than 0.001 were grouped as “Insensitive (/)”, others were grouped as “Sensitive (*)”, shown in column “Sens.” of Table 1.

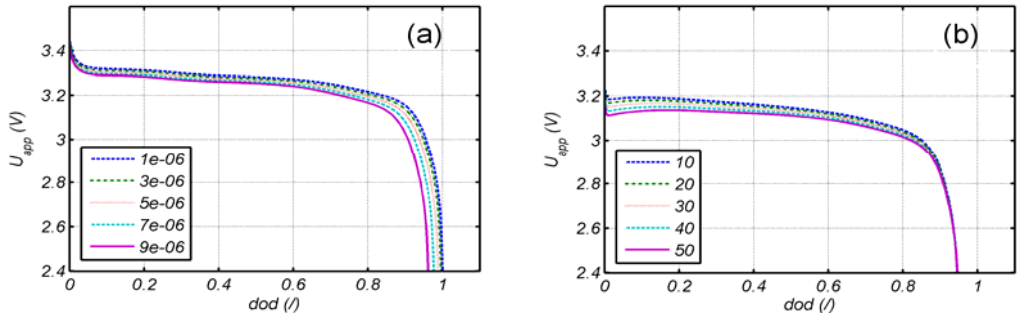

Figure 2: Terminal voltage curve for various value of (a) $R_{s,a}$ at 1C, 25 °C and (b) $\bar{E}k_{s,c}$ at 2C, -5 °C.

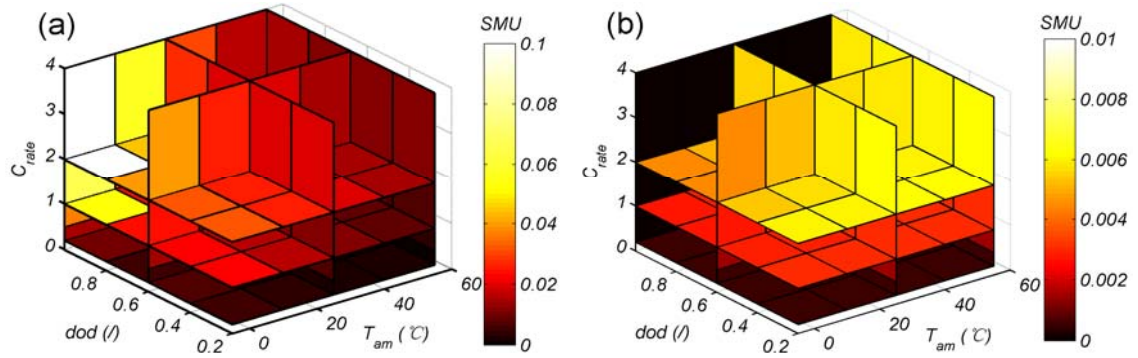

Figure 3: Sensitivity value matrix of parameter (a) $R_{s,a}$ and (b) $R_{film,c}$.

We find that, there is a maximum sensitivity value in each matrix, related to a certain dod, T_{am} and C_{rate}. Theoretically, on this condition the parameter has the greatest sensitivity and can be identified the most easily and accurately. It is named the "Best Condition for Identification (BCI)" indicated by the index of sensitivity value matrix. For example, the "BCI" of parameter $R_{s,a}$ is (5,1,5), means "the highest DOD, lowest temperature and highest discharge rate".

3.3 Cluster analysis

The best identification strategy is identifying each parameter on its "BCI", but it is very complicated even impossible because of the diverse "BCIs" of all parameters. In this case, the parameters which have the same or similar "BCI" should be clustered into one cluster; then they could be identified together on few practicable operating conditions that make them remain sensitive and easy to be identified.

Because "Insensitive" parameters' has little influence on terminal voltage, it is not necessary identify them. Cluster analysis is only taken on those "Highly Sensitive" and "Sensitive" parameters. Fuzzy C-Means method was used for clustering, and the BCI was used as clustering feature. Column "Clusters" in Table 1 shows the parameters' membership to four clusters. Table 2 shows the clustering centers by their index in sensitivity value matrix.

Table 1: Parameters sensitivity analysis and the results of fuzzy clustering

Parameter and unit	bench-mark	Range	SMU_{avg}	Sens.	Clusters			
					A	B	C	D
$R_{s,a}$ (μm)	3.5	1~9	0.0215	**	0.008	0.010	0.978	0.004
$R_{s,c}$ (μm)	0.0365	0.02~0.06	0.0038	*	0.045	0.028	0.910	0.016
$D_{s,a}$ ($m^2\ s^{-1}$)	$3.9\cdot10^{-14}$	$(0.5\sim10)\cdot10^{-14}$	0.0154	**	0.008	0.010	0.978	0.004
$D_{s,c}$ ($m^2\ s^{-1}$)	$1.2\cdot10^{-18}$	$(0.5\sim10)\cdot10^{-18}$	0.0019	*	0.008	0.010	0.978	0.004
$\sigma_{s,a}$ (S m^{-1})	100	10~100	$1.16\cdot10^{-5}$	/	/	/	/	/
$\sigma_{s,c}$ (S m^{-1})	0.5	0.1~5	0.0027	*	0.855	0.026	0.043	0.076
x_0 (/)	0.8	0.75~0.85	0.0159	**	0.078	0.560	0.306	0.056
y_0 (/)	0.03	0.02~0.1	0.0021	*	0.185	0.295	0.123	0.398
$\varepsilon_{s,a}$ (/)	0.55	0.5~0.6	0.0192	**	0.018	0.926	0.038	0.018
$\varepsilon_{s,c}$ (/)	0.43	0.4~0.5	0.0013	*	0.045	0.028	0.910	0.016
$R_{film,a}$ (Ω m^2)	0	0~0.01	0.0034	*	0.008	0.005	0.004	0.984
$R_{film,c}$ (Ω m^2)	0	0~0.01	$2.28\cdot10^{-5}$	/	/	/	/	/
C_e (mol m^{-3})	1200	800~1200	0.0019	*	0.990	0.002	0.004	0.004
D_e ($m^2\ s^{-1}$)	$2\cdot10^{-10}$	$(0.1\sim10)\cdot10^{-10}$	0.0022	*	0.045	0.028	0.910	0.016
κ_e (S m^{-1})	0.2	0.1~2	0.0040	*	0.990	0.002	0.004	0.004
ρ_e (kg m^{-3})	1130	1000~1200	$5.68\cdot10^{-5}$	/	/	/	/	/
R_{ext} (Ω m^2)	0	0~0.002	0.0117	**	0.008	0.005	0.004	0.984
$\varepsilon_{e,a}$ (/)	0.33	0.3~0.4	0.0199	**	0.056	0.749	0.095	0.100
$\varepsilon_{e,s}$ (/)	0.54	0.5~0.6	$7.24\cdot10^{-4}$	/	/	/	/	/
$\varepsilon_{e,c}$ (/)	0.332	0.3~0.4	0.0012	*	0.008	0.010	0.978	0.004
$k_{s,a}$ ($m^{2.5}\ mol^{-0.5}\ s^{-1}$)	$3\cdot10^{-11}$	$(0.1\sim10)\cdot10^{-11}$	0.0414	**	0.427	0.068	0.084	0.422
$k_{s,c}$ ($m^{2.5}\ mol^{-0.5}\ s^{-1}$)	$1.4\cdot10^{-12}$	$(0.1\sim10)\cdot10^{-12}$	0.0142	**	0.990	0.002	0.004	0.004
$\bar{E}k_{s,a}$ (KJ mol^{-1})	20	10~50	0.0044	*	0.874	0.030	0.049	0.046
$\bar{E}k_{s,c}$ (KJ mol^{-1})	30	10~50	0.0014	*	0.990	0.002	0.004	0.004
$\bar{E}D_{s,a}$ (KJ mol^{-1})	35	10~50	0.0019	*	0.008	0.010	0.978	0.004
$\bar{E}D_{s,c}$ (KJ mol^{-1})	35	10~50	$6.94\cdot10^{-4}$	/	/	/	/	/
$\bar{E}D_e$ (KJ mol^{-1})	11	10~50	0.0015	*	0.821	0.034	0.100	0.045
$\bar{E}\kappa_e$ (KJ mol^{-1})	26.6	10~50	0.0085	*	0.990	0.002	0.004	0.004

Table 2: Clustering center (the index in sensitivity value matrix, no unit)

Clusters	$Index_{dod}$	$Index_{Tam}$	$Index_{Crate}$
A	1.1002	1.1715	4.8740
B	4.7931	3.5316	2.4471
C	4.6462	1.0282	4.9632
D	1.0256	4.8243	4.7114

There are 16 parameters belong to cluster A and C, 2 belong to cluster B and 2 belong to cluster D. Other 3 parameters couldn't be clustered clearly because their largest degree of membership is less than 0.6.

We clustered parameter x_0 and y_0 to B and D, due to their largest membership, respectively, and the parameter $k_{s,a}$ can be clustered to both A and D.
From Table 2, the best conditions indicated by cluster A and C are almost the same, one discharge profile which described as “Very low temperature, very high rate” contains both of them. Other two discharge profiles obtained from cluster B and D are “Room temperature, medium rate” and “Very high temperature, very high rate”. The “Best Practicable Conditions (BPC)” for identifying the parameters of $LiFePO_4$ battery can be designed by those three profiles. Furthermore, the detail values of the temperature and discharge rate of “BPC” should be determined according to the battery’s properties and experimental environment.

4. Design criteria and application suggestions of “Best Practicable Conditions”

In order to identify the parameters of the Li-ion battery efficiently and accurately, the “Best Practicable Conditions” should obey following criteria, based on parameter sensitivity analysis.
(1) The “BPC” should contain all “BCIs”. The fewer conditions it contains, the better “BPC” is.
(2) Parameters which to be identified should have their greatest sensitivity on “BPC”, while other parameters’ sensitivity should be lower.
(3) Rough conditions which are harmful to the battery should be avoided in “BPC”.
The suggested directions for future identification using “Best Practicable Conditions” are:
(1) “Insensitive” parameters should be excluded from identification according to the sensitivity analysis, so other parameters could be identified more efficiently and accurately.
(2) “Highly sensitive” parameters should be identified first; the results are used for “Sensitive” parameters’ identification. A step-by-step strategy will improve the identification efficiency.
(3) A global optimization tool (e.g. Generic Algorithm) should be used to speed up the identification.

5. Conclusion

A thermal-electrochemical model of Li-ion battery has been developed based on P2D model by coupling some electrochemical parameters to the battery temperature. Then, 28 parameters were analyzed using sensitivity value matrixes, while 5 “Insensitive” parameters were excluded. Meanwhile, other parameters were clustered into four clusters according to their “BCIs” by FCM method. Finally, the “BPC” for a $LiFePO_4$ battery, which contains three practicable conditions, has been proposed according to the clustering result. It is possible to design a step-by-step identification using this work in the future.

Acknowledgment

This work was supported by the National Science Foundation of China (Grant No. 51107021) and the Fundamental Research Funds for the Central Universities (Grant No. HIT. NSRIF. 2014021).

References

Alexander P.S., Matthias B., Árpád W.I., Lino G., 2010, Experiment-driven electrochemical modeling and systematic parameterization for a lithium-ion battery cell, Journal of Power Sources, 195, 5071-5080.
Joel C.F., Scott J.M., Jeffrey L.S., Hosam K.F., 2012, Genetic identification and fisher identifiability analysis of the Doyle–Fuller–Newman model from experimental cycling of a $LiFePO_4$ cell, Journal of Power Sources, 210, 263-275.
Marc D., Thomas F.F., John N., 1993, Modeling of galvanostatic charge and discharge of the lithium polymer insertion cell, J. Electrochem. Soc., 140, 1526-1533.
Prada E., Di Domenico D., Creff Y., Bernard J., Sauvant-Moynot V., Huet F., 2012, Simplified Electrochemical and Thermal Model of $LiFePO_4$ -Graphite Li-Ion Batteries for Fast Charge Applications, J. Electrochem. Soc., 159, A1508-A1519.
Safari M., Delacourt C., 2011, Modeling of a Commercial Graphite/$LiFePO_4$ Cell, J. Electrochem. Soc., 158, A562-A571.
Srinivasulu G.N., Subrahmanyam T., Rao V.D., 2011, Parametric sensitivity analysis of PEM fuel cell electrochemical Model, International Journal of Hydrogen Energy, 36, 14838-14844.
Wang X.D., Xu J.L., Lee D.J., 2012, Parameter sensitivity examination for a complete three-dimensional, two-phase, non-isothermal model of polymer electrolyte membrane fuel cell, International Journal of Hydrogen Energy, 37, 15766-15777.
Zhang Q., Ralph E.W., 2008, Capacity fade analysis of a lithium ion cell, Journal of Power Sources, 179, 793-798.